Efficient Protection of Mild Steel Corrosion in Hydrochloric Acid Using 3-(5-Amino-1,3,4-thiadiazole-2yl)-2H-chromen-2-one, a Coumarin Derivative Bearing a 1,3,4-thiadiazole Moiety: Gravimetrical Techniques, Computational and Thermodynamic Investigations

W. Khalid Al-Azzawi [1], S. S. Hussein [2], S. M. Salih [2], D. S. Zinad[2], R. K. Al-Azzawi [1], M. M. Hanoon [2], A. A. Al-Amiery [2,3*], M. A. Fayad [2], A. A. H. Kadhum [4], W. N. R. Wan Isahak [3], M. S. Takriff [5]

[1.] Department of Medical Instruments Engineering Techniques, Al-Farahidi University, P. O. Box: 10001, Baghdad, Iraq.

[2.] Materials Engineering Department, University of Technology-Iraq, P. O. Box: 10001, Baghdad, Iraq.

[3.] Department of Chemical and Process Engineering, Faculty of Engineering and Built Environment, Universiti Kebangsaan Malaysia, P. O. Box: 43600, Selangor, Malaysia.

[4.] University of Al-Ameed, P. O. Box: 56001, Karbala, Iraq.

[5.] Chemical and Water Desalination Engineering Program, Department of Mechanical & Nuclear Engineering, Collage of Engineering, University of Sharjah, P. O. Box: 26666, Sharjah, United Arab Emirates.

ABSTRACT

*I*n this study, a novel organic molecule, 3-(5-amino-1,3,4-thiadiazole-2yl)-2H-chromen-2-one (3-ATC), has been investigated for its efficiency in the mild steel corrosion inhibition in 1 M hydrochloric acid solution at various temperatures (303, 313, 323 and 333 K) by gravimetrical analysis. The experimental data showed that 3-ATC is an excellent inhibitor for the corrosion of mild steel in a 1.0 M HCl environment, and the protection performance of 3-ATC is higher than 96 % at 0.0005 M 3-ATC. During adsorption, it was noticed that the 3-ATC exhibits strong inhibitory efficiency, and this phenomenon was discovered to follow the Langmuir adsorption isotherm. Furthermore, the thermodynamic parameters were calculated according to the weight loss findings. The value of free energy of adsorption (ΔG_{ads}) was determined, and it was indicated that chemisorption and physisorption mechanisms are responsible for the adsorption of 3-ATC molecules on mild steel surfaces. In addition, the quantum chemical DFT research was used to study the relationship between the results of inhibitory efficiency and molecule structure. Prog. Color Colorants Coat. 16 (2023), 97-111© Institute for Color Science and Technology.*

1. Introduction

The superior physio-mechanical qualities of mild steel give it the ability to apply in sectors of building and industrial materials. Corrosion damage to metallic materials is a pressing issue that requires prompt attention and understanding from the scientific world to avoid economic and societal consequences. The risk to the plant integrity and lower plant performance is one of the fundamental causes that could affect manufacturing [1]. Acids are widely used in industrial processes, such

as pickling, cleaning, descaling, etc. Inhibitors are effective in reducing the dissolution rate of metals [2]. Mineral acids such as HCl, H_2SO_4, and others are used at temperatures ranging from 60 to 90 degrees Celsius to remove undesired mill scale. These mineral acids are very corrosive, attributed to the prevalence of Cl^- and SO_4^{-2} ions and their corrosiveness must be inhibited by using suitable corrosion prevention measures. The corrosion inhibitors are considered one of the widely efficient techniques to prevent corrosion. An excellent corrosion inhibitor is provided in quite a tiny portion of a corrosive media. It should substitute adsorbed water molecules at the metal substrate and interact with anodic and cathodic sites via their activity from the solution side of the metal/solution interface to adjust electrochemical processes and improve protection against corrosion. Due to corrosion's economic and environmental aspects, the research on corrosion inhibitors becomes essential for long-term investment and strategic relevance. Organic molecules with heteroatoms such as N, S, O, or P, numerous bonds, or aromatic rings have been discovered to be excellent corrosion inhibitors by coordinating to the metal surfaces via the electronic configuration of the Fe atom and these reactive sites in their chemical structure [3-5]. Numerous references are available on developing novel corrosion inhibitors for iron and steel in acidic environments [6-9]. With the highlight of environmental concerns, corrosion inhibitory study has been redirected to molecules with more heteroatoms and practical therapeutic uses in all disciplines [10-12]. The 1,3,4-thiadiazole scaffold has a variety of uses in medicines, agrochemicals, and material science. Therefore, Pharmaceuticals include as following: anti-inflammatory, antihypertensive, anti-HIV, anti-depressant, local anesthetic, and anticonvulsant medications. In addition, it was used to treat various illnesses, and there are currently several compounds in clinical use in the market. It is reported that the Methazolamide is a carbonic anhydrase inhibitor that prevents blindness, nerve damage, and vision loss. Moreover, it treats glaucoma and lowers excessive pressure inside the eyes. Acetazolamide is another medicine used to treat glaucoma, epileptic seizures, dural ectasia, and periodic paralysis [13]. Thiadiazole and its derivatives are excellent candidates for corrosion inhibitors because of a planar aromatic ring, hydrophobicity, and hetero atoms. The previous study [14] mentioned the thiadiazole and its derivative's

corrosion prevention capacity for mild steel and copper in acidic conditions. Figure 1 shows that Coumarin is a broad family of organic extract compounds regarded as an intermediate metabolism in many plants' species, particularly in leaves, seeds, and roots, and is abundant in the Rutaceae and Umbelliferae plant families. It is stated that the Coumarin was discovered in the tonka bean, and its name is derived from the French word coumarou. Coumarin plays a vital role in plant development and metabolite regulation [15]. These Coumarins are separated into simple coumarins, furanocoumarins, pyranocoumarins, and other coumarins based on the different substituents in the overring. It was divided into linear and angular types with the furanocoumarins and pyranocoumarins. It is reported that the natural and synthetic Coumarin derivatives have a wide variety of biological activities, including anti-inflammatory [16], anticancer [17, 18], anti-coagulant, anti-oxidant, anti-HIV, and anti-bacterial [19]. Due to its diverse impacts on diseases and less damage to normal cells, the coumarins' biological activity has become a popular and exciting research topic [20]. Previous research [18-21] has shown that coumarin chalcone fibrates can lower total cholesterol (TC), phospholipids (PL), and triglycerides (TG) while also regulating VLDL, LDL, and HDL levels [21].

Metal corrosion is a big issue that costs billions of dollars annually. The physicochemical interaction between a metal and its environment causes changes in its characteristics, which might change the metal's function. Metal corrosion prevention is critical in metal science due to the widespread use of metals in numerous innovation domains. Although metals are not entirely immune to corrosion, they can be kept safe from corroding to some extent. As a result, corrosion inhibitors are utilized to interact with a metal surface and prevent metal corrosion. The essential materials used are iron metal and its many alloys, which have countless practical applications. Iron is used to build alloys, ships, railroads, bridges, pipes, boilers, reinforcement steel, and other structures.
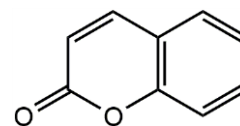
Figure 1: Coumarin chemical structure.

Interestingly, Iron corrosion leads to one-fourth of global production loss in a year, a financial disaster. Therefore, combining the coumarin moiety with the 1,3,4-thiadiazole structure is expected to improve corrosion inhibition. To achieve this goal, we synthesized a coumarin-containing 1,3,4-thiadiazole derivative, namely 3-(5-amino-1,3,4-thiadiazole-2yl)-2H-chromen-2-one (3-ATC) (Figure 2), and tested its corrosion prevention characteristics for mild steel in 1 M HCl using weight loss measurements.

2. Experimental

2.1. Instrumentation and materials

Materials used in this work without further purification are as follows: thiosemicarbazide, 3-carboxycoumarin, and sulfuric acid, which Sigma-Aldrich, Selangor, Malaysia, supplied. Thin-layer chromatography (TLC) was used to check the purity of synthesized inhibitor on silica gel G plate with benzene and methanol 75:25 (v/v) as the mobile phase; the spot was located under ultraviolet light at 254 and 365 nm. The chemical structure of the target compound was characterized by various characterization spectroscopical techniques. The first technique was Fourier transform infrared (FTIR) spectroscopy. The inhibitor spectrum was recorded on an FTIR Spectrometer Thermo Scientific Nicolate 6700 (Thermo Fisher Scientific, Waltham, MA, USA). The second technique was Nuclear magnetic resonance (NMR) spectroscopy, and the synthesized inhibitor spectrum was recorded on AVANCE III 600 MHz spectrometer (Bruker, Billerica, MA, USA).

2.2. Synthesis of tested inhibitor

The synthetic route of the novel 3-(5-amino-1,3,4-thiadiazole-2yl)-2H-chromen-2-one based on 3-carboxycoumarin and thiosemicarbazide consists of one step, as demonstrated in Scheme 1.

An equimolar quantity of an ethanolic mixture of thiosemicarbazide (0.01 mol) and 3-carboxycoumarin (0.01 mol) in the presence of sulfuric acid (5 mL) was prepared. It was refluxed for 7 h, and the resultant was poured on crushed ice. The filtered compound was recrystallized from ethanol to produce the yellow inhibitor with the yield of 74 % and MP 178 °C. The purity of the target compound was confirmed by thin-layer chromatography (TLC). The TLC plate $(20 \times 10$ cm) was recoated silica gel on aluminum 60F–254, with a stationary phase thickness of approximately 0.5 mm. Five microliters of test solution were used on the plate. The TLC plate was placed in a saturated chromatographic tank with a solvent system of benzene-methanol (75:25). FTIR: 3342.9 cm^{-1} (NH$_2$), 3081.3 cm^{-1} (H−CH− aromatic), 1669.3 cm^{-1} (O=C−CO−; lactone), 1607.9 cm^{-1} (C=N), 1545.8 cm^{-1} (−C=C−; methylene group), 1227.2 (-C-O-) and 1131.2 (C-S). ^{1}H-NMR (DMSO-d6): δ 7.24 (2H, dd, $J = 8.3$, for –C=C-H), 7.41 (1H, d, $J = 7.9$, aromatic proton), 7.50 (d, $J = 8.3$, amino protons), and 7.70-7.92 (2H, s, aromatic proton). ^{13}C-NMR (DMSO-d6): δ 165.14 (C=O); 166.02 (S-C=N), 169.51 (N=C-NH$_2$), 153.94 (=C-O-), 137.14 (H-C=C), 130.10 (C aromatic), 128.12 (C aromatic), 127.11 (C aromatic), 125.38 (C aromatic), 118.92 (C aromatic), and 115.21 (C aromatic).
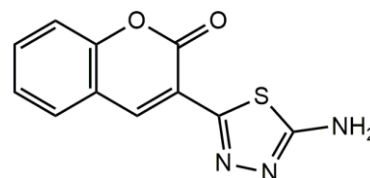
Figure 2: Synthesized inhibitor chemical structure.
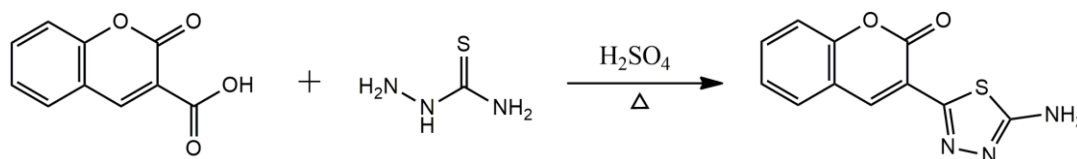
Scheme 1: Synthesis of the novel corrosion inhibitor.

2.3. Corrosion test

2.3.1. Solution

The corrosive solution of 1 M hydrochloric acid was prepared by diluting 37 % HCl with distilled water. The investigated inhibitor concentrations vary from 0.0001 to 0.0005 M, with freshly prepared distilled water, according to the previous work [22].

2.3.2. Metal alloy mild steel

The working electrode's mild steel elemental analysis in weight percent was 0.210 carbon; 0.380 silicon; 0.090 phosphorus; 0.050 manganese; 0.010 aluminum; 0.050 sulphur; and iron balance.

2.3.2. Weight-loss analysis

In the current study, the usual exposure testing approach outlined in NACE TM0169/G31 [23] was obeyed. The gravimetric techniques were conducted out in aerated environments. The investigated mild steel coupons were placed in reaction bottles in the absence and presence of various inhibitor concentrations in 1 M HCl solution. The mild steel coupons ($4.0 \times 2.5 \times 0.5$ cm) were suspended in the corrosive environment for different immersion periods (1, 5, 10, 24, and 48 h) in triplicate. The temperature of solutions was kept at the examined temperature of 303 K in a Thermo Scientific precision water bath. The experiments were repeated for different temperatures (303, 313, 323, and 333 K) and 5 hours as immersion time. The tested inhibitor concentrations were 0.0001, 0.0002, 0.0003, 0.0004, and 0.0005 M. The tested coupons were taken after immersion periods and exposed to the ASTM standard G1-03 [24] post-treatment techniques. The average mass loss (g) was utilized to determine the rate of corrosion [24] according to the Eq. 1.

$$C_R(mm/year) = \frac{87\,600 \times W}{\rho a t} \tag{1}$$

Where; C_R is the corrosion rate, W is the average mass loss (g), ρ is the density (g. cm^{-3}), a is the surface area (cm^2), and t is the exposure time (h).

The inhibition efficiency of the tested inhibitor was calculated based on the following equation (Eq. 2).

$$\%IE = \frac{w_o - w}{w_o} \times 100 \tag{2}$$

Where; $IE\%$ is the percent of inhibition efficiency,

w_o is the average mass losses of the tested coupons in a 1 M HCl environment in the absence of a tested inhibitor, and w is the average mass losses of the tested coupons in 1 M HCl environment in the presence of a tested inhibitor.

2.4. Computational details

The conventional theory addressing Becke's three-parameter hybrid functional (B3LYP) level using Gaussian 03 series with 6–31G as basis set was used to undertake quantum chemistry computations for gas phases utilizing density functional theory (DFT) approaches. The ChemOffice application was used to perform all of the calculations. The relations 3-6 have been used to compute physicochemical characteristics [25], including the energy of the highest occupied molecular orbital energy (E_{HOMO}), the energy of the lowest unoccupied molecular orbital energy (E_{LUMO}), the energy gap $E = E_{HOMO} - E_{LUMO}$ Chemical hardness (η), chemical softness (σ), and electronegativity (χ) (Eqs. 3-6).

$$\Delta E = E_{HOMO} - E_{LUMO} \tag{3}$$

$$\eta = -\frac{E_{HOMO} - E_{LUMO}}{2} \tag{4}$$

$$\sigma = \frac{1}{\eta} \tag{5}$$

$$\chi = -\frac{E_{HOMO} + E_{LUMO}}{2} \tag{6}$$

3. Results and Discussion

3.1. Weight loss measurements

Figure 3 shows the corrosion and corrosion inhibition efficiency rate for mild steel acquired through weight loss measurements without and with the addition of various concentrations of 3-ATC in a 1.0 M HCl environment. The corrosion prevention performance was investigated at 303 K and for different immersion times [26, 27].

The corrosion rate of mild steel corrosion significantly decreased while the protective efficiency increased when the concentration of 3-ATC increased, as shown in Figure 3. The higher inhibitory efficiency is due to the more excellent surface coverage caused by inhibitor molecules adsorbing on the steel surface [28, 29]. The adsorption coating may block the active sites, effectively isolating the examined specimen from the acidic medium. When compared to the thiadiazole

derivatives (or coumarin derivatives) corrosion inhibitors studied earlier (Table 1), it was observed that the 3-ATC gives better performance in terms of corrosion inhibition [30-38].

The present inhibitor (3-ATC) can be compared to other published inhibitors using corrosion inhibitors generated from thiadiazole (or coumarins) to prevent tested coupon surface against corrosion in corrosive media. Table 1 shows that most thiadiazoles tried to have a significant inhibition effect. In comparing the existing inhibitor, 3-ATC has the highest inhibiting performance among the thiadiazole listed in Table 1 [30-35] and an efficacy comparable to that stated in [36-38]. It can be obtained that the increased concentration of 3-ATC leads to a significantly decreased rate of corrosion as well as the corrosion inhibition efficiency enhanced due to an increase in the inhibitor's adsorption coverage on mild steel surfaces as the 3-ATC concentration rises. The improvement in surface coverage due to the adsorption of inhibitor molecules on the steel substrate can justify the gain in protective efficiency. The adsorbed barrier then protects the steel substrate from the corrosive medium by blocking the active sites. Compared to the first tested thiadiazole inhibitors in Table 1, 3-ATC demonstrated superior protection from corrosion. The influences of steric hindrance and substituents in the inhibitor molecules are linked to this phenomenon. The best inhibiting effectiveness was observed once the inhibitor was introduced to the corrosive media at a concentration of 3-ATC was 0.0005 M. In contrast, it was found that the inhibiting efficacy did not change much when the concentration increased to 0.001 M 0.001 M.

3.2. Effect of immersion time

According to the weight loss data, the inhibitory efficiency improved as the concentration and immersion time increased. After 5 hours of exposure, it was obtained that the most excellent corrosion inhibition efficiency by around 93 % at 0.0005 M concentration. There is no significant increase after 5 hours of immersion in corrosion inhibition efficiency, while the inhibition efficiency declines after 24 hours due to the desorption of the studied inhibitor from the tested coupon surface and to the instability of the protective layer on the coupon surface [39]. Furthermore, a significant decrease in inhibitory efficiency was noticed after 48 hours of exposure.
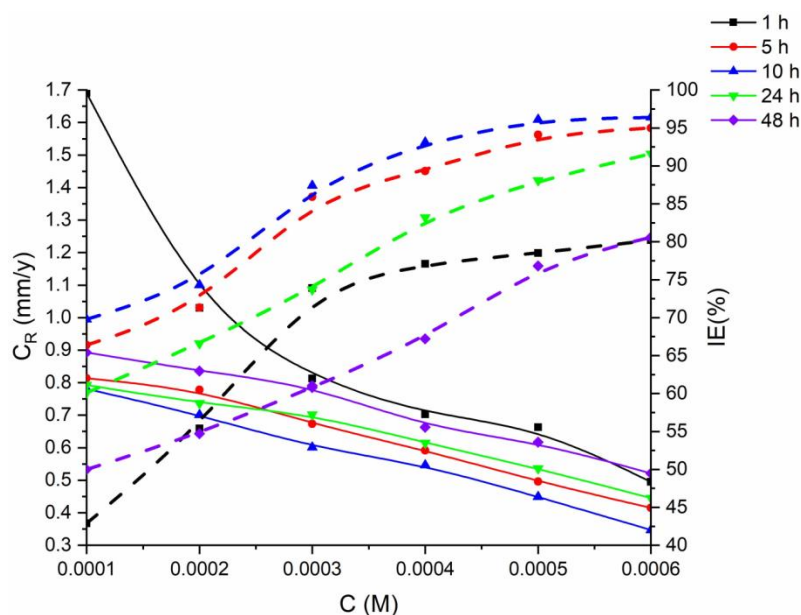
Figure 3: Weight loss measurements data of mild steel coupon in 1.0 M HCl with different inhibitor concentrations at 303 K and various exposure periods.

Table 1: The inhibiting performance of 3-ATC was compared objectively to that of other thiadiazole derivatives (or coumarin derivatives) that had been studied lately.

Inhibitor	Corrosive solution	Inhibitor concentration	%IE	Ref.
3-ATC	1 M HCl	0.0005 M	96	-
5,5′-(1,4-phenylene)bis(N,N-diphenyl-1,3,4-thiadiazol-2-amine)	1 M HCl	0.5 mM	94	30
N,N′-(1,4-phenylenebis(methanylylidene))bis(5-(methylthio)-1,3,4-thiadiazol-2-amine) (PMTTA),	1 M HCl	125 ppm	92.6	31
5,5′-((1,4-phenylenebis(methanylylidene))bis(azanylylidene))bis(1,3,4-thiadiazole-2-thiol) (PATT),	1 M HCl	125 ppm	90.9	31
N,N′-(1,4-phenylenebis(methanylylidene))bis(5-methyl-1,3,4-thiadizol-2-amine) (PMTA)	1 M HCl	125 ppm	87.7	31
N,N′-(1,4-phenylenebis(methanylylidene))bis(1,3,4-thiadiazol-2-amine) (PTA)	1 M HCl	125 ppm	80.3	31
3-(4-methoxyphenyl)-3,4-diphenyl-2,3-dihydro-1,2,5-thiadiazole 1,1-dioxide (TANIS)	0.5 M H$_2$SO$_4$	60 μM	76	32
4-(1,1-dioxido-3,4-diphenyl-2,3-dihydro-1,2,5-thiadiazol-3-yl)-N,N-dimethylaniline (TDMA)	0.5 M H$_2$SO$_4$	60 μM	82	32
5-[(2-(3,4,5-trimethoxyphenyl)-6-phenylimidazo [2,1-b][1,3,4]thiadiazol5-yl) methylidene]-1,3-thiazolidine2,4-dione	15 % HCl	200 ppm	88	33.
5-[2-(3,4,5-trimethoxyphenyl)-6-(4-methoxylphenyl)-imidazo[2,1-b][1,3,4] thiadiazol-5-yl)methylidene]- 1,3-thiazolidine-2,4-dione	15 % HCl	200 ppm	93	33.
(Z)-5-(4-chlorobenzylidene)-3-(benzo[d] thiazol-2-yl)- 2-(4-methoxyphenyl) thiazolidine-4-one	15 % HCl	50 ppm	86	34.
(Z)-5-(4-methoxybenzylidene)-3-(benzo[d]thiazol2- yl)-2-(4-methoxyphenyl) thiazolidine-4-one	15 % HCl	50 ppm	91	34.
2-Amino-5-(4-methoxyphenyl)-1,3,4-thiadiazole (AMPT)	15 % HCl	200 ppm	82	35.
2-Amino-5-phenyl-1,3,4-thiadiazole (APT)	15 % HCl	200 ppm	79	35
2-Amino-5-(4-chlorophenyl)-1,3,4-thiadiazole (ACPT)	15 % HCl	200 ppm	75	35
4-((4-amino-5-thio-1,2,4-triazol-3-yl)methyl)coumarin (ATTC)	1 M HCl	0.5 mM	96	36
2-4(difuran-2-yl-3-azabicyclo[3.3.1] nonan-9-yl-)-5-spiro-4-acetyl-2-acetylamino-1,3,4-thiadiazoline (DFAT)	15 % HCl	50 ppm	96	37
2-4(di-1H indole-3-yl-3-azabicyclo[3.3.1]nonan-9-yl-)-5-spiro-4-acetyl-2-acetylamino-1,3,4-thiadiazoline (DIAT)	15 % HCl	50 ppm	97	37
3-[(5-phenyl-1,3,4-thiadiazole-2- ylimino)methyl]quinoline 2-ol(SB1)	1 M H$_2$SO$_4$	0.5 mM	95	38
3-[(5-phenyl-1,3, 4-thiadiazole-2-ylimino)methyl]quinoline 2-thiol (SB 2)	1 M H$_2$SO$_4$	0.5 mM	96	38

3.3. Effect of temperature

Figure 4 shows the impact of temperatures on corrosion rate and inhibitive performance in 1 M HCl at temperatures ranging from 303 to 333 K in the absence and presence of different inhibitor doses. The best immersing period (10 hours) was chosen based on the best inhibitory effectiveness found when all concentrations were compared. The protective efficacy decreased as the temperature increased from 303 to 333 K. This phenomenon might be explained by the desorption of adsorbed inhibitor molecules on the coupon surface. As a result of the inhibitor adsorption on the steel surface, inhibition happens, and raising the temperature will facilitate the desorption of inhibitor

molecules from the coupon surface [40].

The corrosion process activation parameters were determined according to Arrhenius (Eq.1):

$$\log C_R = \log K - \left[\frac{E_a}{2.303RT}\right] \tag{7}$$

Where; K is the frequency parameter, E_a is the activation energy, R is the gas constant, and T is the temperature.

Figure 5 between $\log C_R$ and $1/T$ [34] was used to calculate the activation energy for mild steel in 1 M HCl without and with the addition of various inhibitor concentrations. Figure 5 depicts a straight line with a slope of $\frac{E_a}{2.303R}$ that was used to compute the E_a and show it in Table 2. The adsorption of inhibitor molecules on the tested coupon surface decreases as temperature rises, increasing the corrosion rate. For high temperatures, the rate of corrosion rate increases as the adsorption of inhibitor molecules on the mild steel surface decreases.
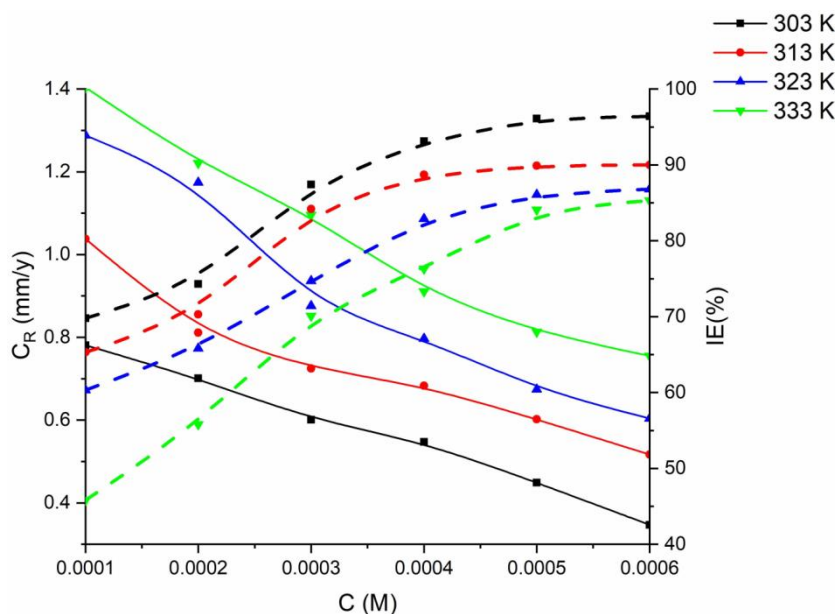
Figure 4: Weight loss measurements data of tested coupon in 1.0 M HCl with different inhibitor concentrations.
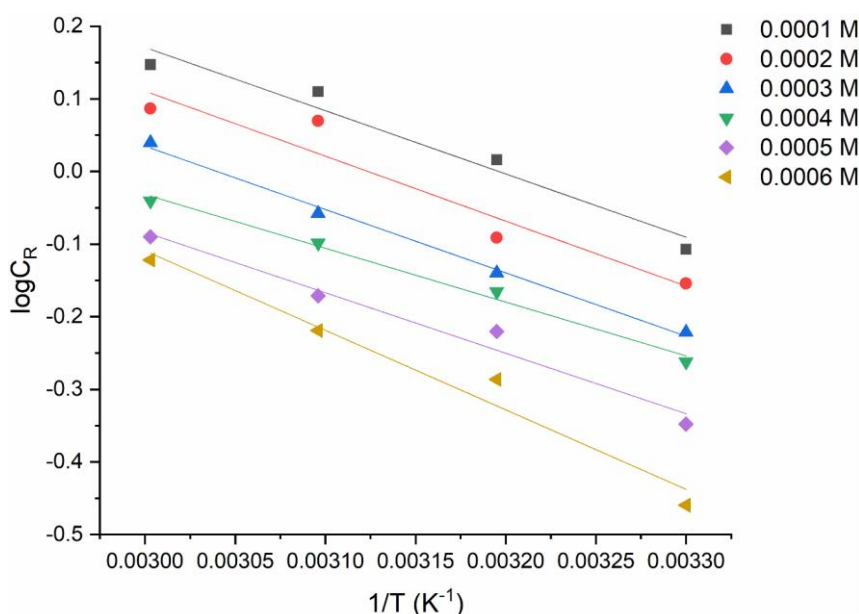
Figure 5: The $\log C_R$ vs $1/T$ for the different concentrations of 3-ATC and various temperatures.

Table 2: The values of activation parameters for tested coupon in 1 M HCl environment without and with the addition of various concentrations of 3-ATC and different immersion times.

C (M)	E_a ($kJ.mol^{-1}$)		
	5 (h)	**10 (h)**	**4h (h)**
Blank	55.93	55.91	55.32
0.0001	47.48	45.74	49.39
0.0002	44.58	43.88	48.01
0.0003	42.95	41.04	45.33
0.0004	39.53	37.90	44.13
0.0005	31.28	30.43	42.11
0.0006	28.84	28.02	41.73

Because the values of activation energies for inhibited environments are greater than those for uninhibited environments, tested coupon surface dissolving is gradual. It is also shown that activation energy values increase as the concentration of the tested inhibitor rises, indicating that there is an energy barrier in the presence of the tested inhibitor, which increases as the tested inhibitor concentration increases. At increasing temperatures, the adsorption of inhibitor molecules on the tested coupon surface decreases, resulting in a proportional increase in the corrosion rate.

According to equation a modified Arrhenius plot of $logC_R/T$ against $1/T$ for mild steel dissolution in 1 M HCl allows the values of the enthalpy of activation (ΔH_a) and the entropy of activation (ΔS_a) to be determined.

$$\log\left[\frac{C_R}{T}\right] = \left\{\left[\log\left(\frac{R}{Nh}\right) + \left(\frac{\Delta S_a}{2.303R}\right)\right] - \left(\frac{\Delta H_a}{2.303RT}\right)\right\} \tag{8}$$

Where; N and h represents Avogadro's number and Plank's constant, respectively.

A plot of $logC_R/T$ versus $1/T$ is demonstrated in Figure 6. The activation enthalpy and entropy values have been determined from the slope and intercept of Figure 6 and presented in Table 3. The mild steel dissolution endothermic parameter is reflected by the activation enthalpy positive values (32.53-28.52 kJ.mol^{-1}). The reduction in corrosion rate depends on the kinetic characteristics of activation, as indicated in the results that the activation enthalpy decreases with increasing temperature.

Table 3: The values of isothermal parameters for mild steel in 1 M HCl without and with the addition of 0.0005 M of the tested inhibitor at various temperatures.

T (K)	ΔH_a (kJ. mol^{-1})	ΔS_a (J. mol^{-1}K^{-1})
303	32.53	-121.52
313	31.75	-132.64
323	29.94	-144.76
333	28.52	-151.36
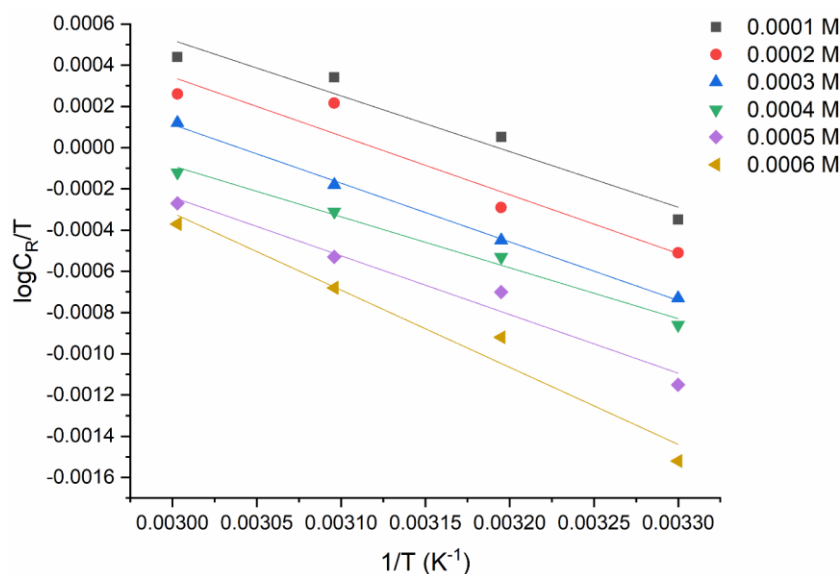
Figure 6: An Arrhenius graph of $log C_R/T$ against $1/T$ for mild steel without and with the addition of the investigated inhibitor.

From the slope of Figure 6, the enthalpy of activation values without and with the addition of the investigated inhibitor was 55.38 and 32.53 kJ.mol^{-1}, respectively. At 303 K and in the absence and presence of the examined inhibitor, the values of activation entropy were -169.83 and -121.52 J.mol^{-1}K^{-1}, respectively. The mild steel dissolving process is endothermic, according to positive ΔH_a Values without and with the addition of the investigated inhibitor [35, 36].

3.4. Adsorption isotherm

Generally, the ability of 3-ATC molecules to be adsorbed on the mild steel surface determines their inhibitory effectiveness. As a result, it is critical to comprehend the adsorption isotherm, which provides crucial information on the inhibitor molecules' interactions with the surface of the metal. The nature and chemical composition of the inhibitor molecules and how they are adsorbed on the surface (physical and chemical adsorptions) influence the corrosion-inhibiting mechanism of mild steel surfaces [37]. The inhibitor concentration and surface coverage (θ) were studied using several adsorption models to determine the best adsorption isotherm. In 1 M HCl solution, the equilibrium adsorption of the tested inhibitor fits the Langmuir adsorption model on the iron surface. According to Equation 9, surface coverage is related to inhibitor concentration and equilibrium constant (K_{ads}) using the Langmuir model.

$$\frac{C}{\theta} = \frac{1}{K_{ads}} + C \tag{9}$$

The value of the linear correlation coefficient (R^2) was found to be close to unity when plotting $\frac{C}{\theta}$ versus C, as shown in Figure 7, indicates that the adsorption process of tested inhibitor molecules in acidic solution on a mild steel surface obeys the adsorption model of Langmuir. Equation 10 [38] was used to calculate the ΔG^o_{ads} value:

$$\Delta G^o_{ads} = -2.303 \ RT \ log55.5K_{ads} \tag{10}$$

Where; R is the constant of gas, T is the temperature, and the number 55.5 is the water concentration in a molar.

Previous research has shown that if the value of $\Delta G°_{ads}$ is negative, the inhibitor molecules' adsorption on the metal surface is a spontaneous process [39]. The value of $\Delta G°_{ads}$ for the tested inhibitor in this study is 37.29 kJ.mol^{-1} (at 303 K), implying that the adsorption mechanism is governed by physisorption and chemisorption [40, 41].

3.5. Quantum chemical studies

The density functional theory with B3LYP at the basis set 6–31G* was used to do quantum chemical computations. Table 4 shows the quantum parameters that have been proposed. Frontier MO energies, such as E$_{HOMO}$ and E$_{LUMO}$, are crucial in predicting reactive

chemical species. The ability to donate an electron is frequently connected with E_{HOMO}, as depicted in Figure 8. As a result, a rise in E_{HOMO} suggests a stronger proclivity to donate electrons to the proper acceptor with an unoccupied orbital. The high value of E_{HOMO} makes it easier for protective particles to absorb onto the metal surface. The inhibitor's protecting performance was improved by boosting the adsorbent film's transport process [42-44]. The acquired quantum chemical data validates according to both physical and chemical adsorption processes [45, 46]. The negative value of E_{HOMO}, and other thermodynamic features, confirm that the quantum chemical data is in good agreement with physisorption and chemisorption mechanisms. Because the energy gap is related to the inhibitor molecules' softness and/or hardness, previous investigations have

shown that ΔE with a high value implies that the inhibitor molecules have poor reactivity [47-50]. A smaller energy gap of a soft molecule leads to less reactive than a hard one. The ΔE value, in addition to the value of dipole moment (μ) indicates that the studied inhibitor molecules have considerable inhibitory effectiveness as corrosion prevention for steel specimens in a 1 M HCl environment.

Many scientists believe heteroatoms with a strong negative charge can be adsorbed on the mild steel surface via the donors-acceptors reaction process [51-53]. Moreover, a low electronegativity and a low value of high molecular weight promote efficient adsorption of tested inhibitor molecules on the mild steel surface, lowering the corrosion rate.

Table 4: Electronic characteristics of 3-ATC evaluated DFT.

Inhibitor	E_{HOMO} eV	E_{LUMO} eV	ΔE eV	η	σ	χ	μ
3-ATC	-8.161	-4.706	-3.455	1.7275	0.5788	6.4335	5.018
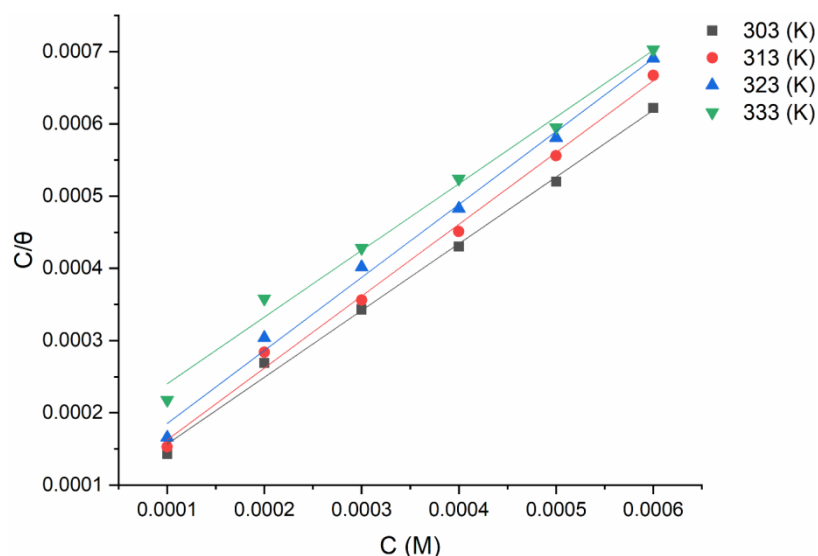
Figure 7: The plot of the adsorption model of Langmuir for the adsorption of 3-ATC molecules in 1 M HCl on coupon surface between the temperature 303 to 333 K.
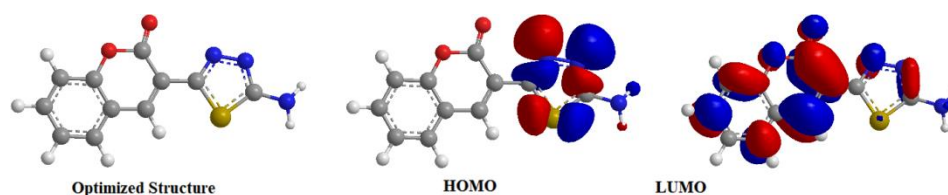
Figure 8: The electronic structures of 3-ATC.

3.6. Proposed corrosion inhibition mechanism

The corrosion of mild steel in hydrochloric acid solution is essentially uniform. When a sample of mild steel is dipped into a hydrochloric acid environment, an attack on the mild steel occurs due to the formation of ferrous ionic species (Fe^{2+}) and hydrogen generation. The steps that were followed were used to describe this mechanism. The following equations (Eqs. 11-16) show how anodic dissolution works.

$$Fe + H^+ + e^- \rightarrow FeH \tag{11}$$

$$FeH + FeH \rightarrow 2Fe + H_2 \tag{12}$$

$$H_2O_{(ads)} \rightarrow OH^-_{(ads)} + H^+_{(aq)} \tag{13}$$

$$Fe + OH^-_{(ads)} \leftrightarrow FeOH_{(ads)} + e^- \tag{14}$$

$$FeOH_{(ads)} \rightarrow FeOH^+ + e^- \tag{15}$$

$$FeOH^+ + H^+ \leftrightarrow Fe^{++} + H_2O \tag{16}$$
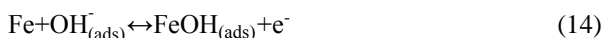
In addition, the following equations determine cathodic H_2 development (Eqs. 17-19):

$$Fe + H^+_{(ads)} \leftrightarrow FeH^+_{(ads)} \tag{17}$$

$$FeH^+_{(ads)} + e^- \leftrightarrow FeH_{(ads)} \tag{18}$$

$$FeH_{(ads)} + H^+ + e^- \leftrightarrow Fe + H_2 \tag{19}$$
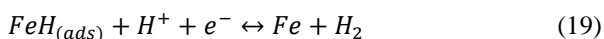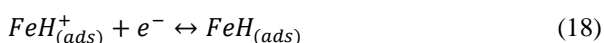
Unfortunately, the mechanism of the inhibition technique was explained by heterocyclic molecules. It was investigated regarding adsorption of heterocyclic molecules at the metal/solution interface, based on the results obtained from weight loss methods. It is indicated that the assessment of heterocyclic molecules behaves as an ingenious inhibitor of corrosion of mild steel in 1.0 M HCl solution, as well as previously described investigations [44-48]. The physical or chemical adsorption mechanism or a combination of the two adsorption mechanisms can be used in the adsorption process. The thermodynamic parameters of the present report indicated that the nature of adsorption of the inhibitor on the surface of mild steel in HCl solution was mostly physical and chemical. The adsorption of inhibitor molecules to the surface of mild steel was determined by the chemical compositions, the charge density strength, and the acidic environment's nature. The chemical structures of the tested heterocyclic molecule examined (Figure 1) show that they display a variety of adsorption mechanisms [49-52], which can be described as follows:

First, portions of heterocyclic molecules were protonated in an acidic solution [53-55]. It results in the coexistence of protonated cations with neutral heterocyclic molecules. The electrostatic interaction between the proton inhibitor molecules and the surface of positively charged mild steel depends on consideration. Conversely, in the HCl environment, the originally adsorbed negatively charged chloride anions (Cl^-) are stretched to conform to the surface of the positively charged steel, resulting in an excess negative charge on the steel surface [56-58]. As a result of the electrostatic attraction between the negatively charged surface and the proton inhibitor particles, a protective barrier will form on its surface (physical adsorption). Second, the creation of coordination bonds between lone electron pairs placed on oxygen and nitrogen in heterocyclic molecules, and the unoccupied d orbitals of iron atoms, may lead to adsorption of tested heterocyclic molecules [59-62]. Figure 9 represents the suggested inhibition mechanism of tested corrosion inhibitor and mild steel in an acidic environment.
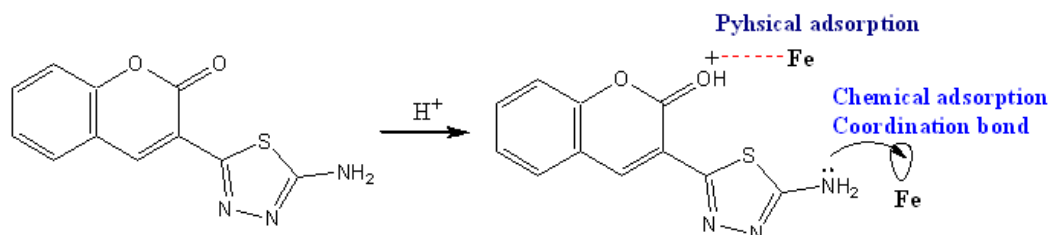
Figure 9: The suggested inhibition mechanism of the tested inhibitor for mild steel surface.

Moreover, the electrons in the aromatic rings of the investigated Schiff base molecules can adsorb via an acceptor-donor interaction (chemical adsorption). Thirdly, the studied dye compounds are excellent ligands forming coordination complexes by chelating with metal ions. As a result, they may form metal–inhibitor complexes $[Fe^{++} - Inh]_{(ads)}$ with Fe^{++} ions produced on the mild steel surface, creating a blocking barrier to further dissolution according to the equation 20.

$$Inh_{(ads)} + Fe^{+++} \rightarrow [Fe^{++} - Inh]_{(ads)} \qquad (20)$$
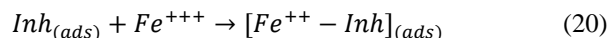
As shown in the equation, the adsorption of inhibitor molecules also entails replacing one or more water molecules adsorbed on the metal surface with these same molecules or anions of acidic solutions (Eq. 21).

$$Inh_{(sol)} + xH_2O_{(ads)} \rightarrow Inh_{(ads)} + xH_2O_{(sol)} \qquad (21)$$
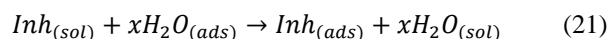
Finally, iron is oxidized in hydrochloric acid solution, forming an iron salt (FeCl$_2$) with the release of $H_2 \uparrow$, as shown in the equation 22.

$$HCl+Fe \rightarrow FeCl_2+H_2 \uparrow \qquad (22)$$

The FeCl$_2$ generated is less soluble and adheres tightly to the surface of mild steel, forming a protective layer that protects the surface of mild steel from additional hydrochloric acid attacks [59-62].

4. Conclusion

The main conclusions drawn from this study are:

1. A coumarin derivative, 3-(5-amino-1,3,4-thiadiazole-2yl)- 2H-chromen-2-one (3-ATC), has been synthesized in one reaction step. The chemical structure of 3-ATC was then elucidated by FTIR, ^{1}H-NMR, and ^{13}C-NMR spectroscopies in addition to CHN-micro elemental techniques.

2. It can be concluded that the 3-ATC has significant corrosion inhibition efficiency for mild steel in 1 M HCl solution.

3. Mass loss experiments demonstrated that increasing the 3-ATC concentration increases the protective efficacy value and reduces the corrosion rate value.

4. The experimental data showed that 3-ATC is an excellent inhibitor for the corrosion of mild steel in a 1.0 M HCl environment, and the protection performance of 3-ATC is higher than 96 % at 0.0005 M 3-ATC.

5. The adsorption of 3-ATC molecules on a mild steel surface was observed following the Langmuir isotherm model.

6. Quantum computations suggested that the inhibition effect of 3-ATC molecules increased with an increase in E_{HOMO} value and a reduction in the ΔE value. The theoretical results obtained from density functional theory computations agreed with the mass loss analysis findings.

7. The adsorption of 3-ATC molecules on the mild steel surface may be due to the coordination bonds between the unpaired electrons of heteroatoms and the unoccupied d-orbital of Fe-atoms located on the mild steel surface (chemical adsorption) and also via the van der Waals interactions between the inhibitor molecules and the mild steel surface.

5. References

1. F. Heakal, A. E. Elkholy, Gemini surfactants as corrosion inhibitors for carbon steel, *J. Mol. Liq.*, 230(2017), 395-407.

2. F. Heakal, A.S. Fouda, M.S. Radwan, Inhibitive effect of some thiadiazole derivatives C-steel corrosion in neutral sodium chloride solution, *Mater. Chem. Phys.*, 125 (2011), 26-36.

3. E. Ochoa, S.J. Jiménez, J. Hernández, T. Pandiyan, J.M. Vásquez-Pérez, J. Borbolla, Benzimidazole ligands in the corrosion inhibition for carbon steel in acid medium: DFT study of its interaction on Fe30 surface, *J. Mol. Str.*, 1119(2016), 314-324.

4. M.A. Hegazy, A.Y. El-Etre, M. El-Shafaie, K.M. Berry, Novel cationic surfactants for corrosion inhibition of carbon steel pipelines in oil and gas wells applications, *J. Mol. Liq.*, 214(2016), 347-356

5. M. Messali, H. Lgaz, R. Dassanayake, R. Salghi, S. Jodeh, N. Abidi, O. Hamed, Guar gum as efficient non-toxic inhibitor of carbon steel corrosion in phosphoric acid medium: Electrochemical, Surface, DFT and MD simulations studies, *J. Mol. Str.*, (2017), 43-54.

6. M. A. Migahed, M. M. EL-Rabiei, H. Nady, H. M. Gomaa, E. G. Zaki, Corrosion inhibition behavior of synthesized imidazolium ionic liquids for carbon steel in deep oil wells formation water, *J. Biol. Tribo Corros.*, 3(2017), 1-20

7. Y.E. Louadi, F. Abrigach, A. Bouyanzer, R. Touzani,

A. El Assyry, A. Zarrouk, B. Hammouti, Theoretical and experimental studies on the corrosion inhibition potentials of two Tetrakis Pyrazole derivatives for mild steel in 1.0 M HCl, *Portugaliae Electrochim. Acta*, 35(2017), 159-178

8. M. E. Mashuga, L. O. Olasunkanmi, E. E. Ebenso, Experimental and theoretical investigation of the inhibitory effect of new pyridazine derivatives for the corrosion of mild steel in 1 M HCl, *J. Mol. Str.*, 1136(2017), 127-139

9. T. Sasikala, K. Parameswari, S. Chitra, A. Kiruthika, Synthesis and corrosion inhibition study of benzodiazepines on mild steel in sulphuric acid medium, *Measurement*, 101(2017), 175-182

10. F. Bentiss, M. Traisnel, M. Lagrenee, The substituted 1,3,4-oxadiazoles: a new class of corrosion inhibitors of mild steel in acidic media, *Corros. Sci.*, 42(2000), 127-146

11. H. Lgaz, R. Salghi, S. Jodeh, B. Hammouti, Effect of clozapine on inhibition of mild steel corrosion in 1.0 M HCl medium, *J. Mol. Liq.*, 225 (2017), 271-280

12. H.L.Y. Sin, M. Umeda, S. Shironita, A.A. Rahim, B. Saad, Adenosine as corrosion inhibitor for mild steel in hydrochloric acid solution, *Res. Chem. Intermed.*, 43(2017), 1919-1934

13. X. Han, Y. L. Yu, Y. S. Hu, X. H. Liu. 1,3,4-thiadiazole: a privileged scaffold for drug design and development, *Curr Top Med Chem.*, 21(2021), 2546-2573.

14. R. Kenchappa, Y. D. Bodke, S. Telkar, M.A. Sindhe, Antifungal and anthelmintic activity of novel benzofuran derivatives containing thiazolo benzimidazole nucleus: an in vitro evaluation, *J. Chem. Biol.*, 10(2017), 11-23

15. M. A. Musa, J.S. Cooperwood, M.O.F. Khan, A review of coumarin derivatives in pharmacotherapy of breast cancer, *Current Medicinal Chem.*, 15(2008), 2664-2679.

16. A. Witaicenis, L.N. Seito, A. da Silveira Chagas, L.D. de Almeida Junior, A.C. Luchini, P. Rodrigues-Orsi, Antioxidant and intestinal anti-inflammatory effects of plant-derived coumarin derivatives, *Phytomedicine*, 21(2014), 240-246.

17. T. Nasr, S. Bondock and M. Youns, Anticancer activity of new coumarin substituted hydrazide–hydrazone derivatives, *Eur. J. Medicinal Chem.*, 76(2014), 539-548.

18. J. Bronikowska, E. Szliszka, D. Jaworska, Z.P. Czuba and W. Krol, The coumarin psoralidin enhances anticancer effect of tumor necrosis factor-related apoptosis-inducing ligand (TRAIL), *Molecules*, 17(2012), 77-89.

19. C. Canning, S. Sun, X. Ji, S. Gupta and K. Zhou, Antibacterial and cytotoxic activity of isoprenylated coumarin mammea A/AA isolated from Mammea africana, *J. Ethnopharmacology*, 147(2013), 259-262.

20. H. Murat Bilgin, M. Atmaca, B. Deniz Obay, S. Özekinci, E. Taşdemir and A. Ketani, Protective effects of coumarin and coumarin derivatives against

carbon tetrachloride-induced acute hepatotoxicity in rats, *Exp. Tox. Path.*, 63(2011), 325-330.

21. K.V. Sashidhara, G.R. Palnati, R. Sonkar, S.R. Avula, C. Awasthi and G. Bhatia, Coumarin chalcone fibrates: A new structural class of lipid lowering agents, Eur. J. Medicinal Chem., 64(2013), 422-431.

22. H. Sorkhabi, M. Majidi, K. Seyyedi, Investigation of inhibition effect of some amino acids against steel corrosion in HCl solution, *Appl. Surf. Sci.*, 2(2004), 176-185.

23. NACE International, Laboratory Corrosion Testing of Metals in Static Chemical Cleaning Solutions at Temperatures below 93 C (200 F), TM0193-2016-SG, 2000 .

24. ASTM International, Standard Practice for Preparing, Cleaning, and Evaluating Corrosion Test, (2011), 1-9.

25. T. Koopmans, Ordering of wave functions and eigenenergies to the individual electrons of an atom, *Physica*, 1(1933), 104-113.

26. R. Salim, N. Betti, M. Hanoon, A. Al-Amiery, 2-(2, 4-Dimethoxybenzylidene)-N-phenylhydrazinecarbothioamide as an efficient corrosion inhibitor for mild steel in acidic environment, *Prog. Color Colorants Coat.*, 15(2022), 45-52.

27. L. Shaker, A. Al-Adili, A. Al-Amiery, Takriff, The inhibition of mild steel corrosion in 0.5 M H_2SO_4 solution by N-phenethylhydrazinecarbothioamide (N-PHC). In Journal of Physics: Conference Series; IOP Publishing: Bristol, UK, 1795(2021), 012009.

28. A. Alamiery, A. Mohamad, A. Kadhum, M. Takriff, The synergistic role of azomethine group and triazole ring at improving the anti-corrosive performance of 2-amino-4-phenylthiazole, *South Afr. J. Chem. Eng.*, 38(2021), 41-53.

29. A. Al-Amiery, L. Shaker, A. Kadhum, M. Takriff, Synthesis, characterization and gravimetric studies of novel triazole-based compound, *Int. J. Low-Carbon Technol.*, 15(2020), 164-170.

30. Salman, Q. Jawad, K. Ridah, L. Shaker, A. Al-Amiery, Selected bis-thiadiazole: synthesis and corrosion inhibition studies on mild steel in HCl environment, *Surf. Rev. Lett.*, 27(2020), 2050014.

31. S. Vinodhini, J. Xavier, Effect of graphene oxide wrapped functional silicon carbide on structural, surface protection, water repellent, and mechanical properties of epoxy matrix for automotive structural components, *Colloids Surfaces A: Physicochem. Eng. Asp.*, 639(2022), 128300.

32. A. Grillo, N. R. Arroyo, M. J. Banera, M. V. Mirífico, 1,2,5-Thiadiazoline S,S-dioxide derivatives as corrosion inhibitors for mild steel in sulphuric acid solution. Electrochemical studies and cytotoxic effect evaluation, *New J. Chem.*, 45(2021), 6950-6959.

33. M. Yadav, D. Behera, S. Kumar, P. Yadav, Experimental and quantum chemical studies on corrosion inhibition performance of thiazolidinedione derivatives for mild steel in hydrochloric acid solution, *Chem. Eng. Commun.*, 202(2015), 303-315.

34. M. Yadav, S. Kumar, N. Kumari, I. Bahadur, E. E. Ebenso, Experimental and theoretical studies on corrosion inhibition effect of synthesized benzothiazole derivatives on mild steel in 15% HCl solution, *Int. J. Electrochem. Sci.*, 10(2015), 602-624.

35. M. Yadav, Sumit Kumar, Debasis Behera, Inhibition effect of substituted thiadiazoles on corrosion activity of N80 steel in HCl Solution, *J. Metallurgy*, 2013(2013),1-14.

36. T. Salman, Q. Jawad, M. Hussain, A. Al-Amiery, L. Shaker, A. Kadhum, M. Takriff, R. Hussain, New environmental friendly corrosion inhibitor of mild steel in hydrochloric acid solution: Adsorption and thermal studies, *Cogent Eng.*, 7(2020), 1826077.

37. N. Tiwari, R. K. Mitra, M. Yadav, Corrosion protection of petroleum oil well/tubing steel using thiadiazolines as efficient corrosion inhibitor: Experimental and theoretical investigation, *Surf. Interfaces*, 22(2021), 100770.

38. P.M. Dasami, K. Parameswari, S. Chitra, Corrosion inhibition of mild steel in 1MH2SO4 by thiadiazole Schiff bases, *Measurement*, 69(2015), 195-201

39. S. Al-Taweel, K. Al-Janabi, H. Luaibi, A. Al-Amiery, T. Gaaz, Evaluation and characterization of the symbiotic effect of benzylidene derivative with titanium dioxide nanoparticles on the inhibition of the chemical corrosion of mild steel, *Int. J. Corros. Scale Inhib.*, 8(2019), 1149-1169.

40. A. Nahlé, R. Salim, F. El Hajjaji, M. Aouad, M. Messali, F. Ech-Chihbi, B. Hammouti, M. Taleb, Novel triazole derivatives as ecological corrosion inhibitors for mild steel in 1.0 M HCl: Experimental & theoretical approach, *RSC Adv.*, 11(2021), 4147-4162.

41. T. Salman, A. Al-Amiery, L. Shaker, A. Kadhum, M. Takriff, A study on the inhibition of mild steel corrosion in hydrochloric acid environment by 4-methyl-2-(pyridin-3-yl) thiazole-5-carbohydrazide, *Int. J. Corros. Scale Inhib.*, 8(2019), 1035-1059.

42. H. Habeeb, H. Luaibi, A. Abdullah, M. Dakhil, A. Kadhum, A. Al-Amiery, A.A. Case study on thermal impact of novel corrosion inhibitor on mild steel, *Case Stud. Therm. Eng.*, 12 (2018), 64-68.

43. M. Quraishi, H. Sharma, 4-Amino-3-butyl-5-mercapto-1, 2, 4-triazole: A new corrosion inhibitor for mild steel in sulphuric acid, *Mater. Chem. Phys.*, 78(2003), 18-21.

44. T. Poornima, J. Nayak, A. Shetty, Corrosion inhibition of the annealed 18 Ni 250 grade maraging steel in 0.67 m phosphoric acid by 3, 4-dimethoxybenzaldehyde thiosemicarbazone, *Chem. Sci. J.*, 69(2012), 1-13.

45. M. Abdallah, E. Helal, A. Fouda, Aminopyrimidine derivatives as inhibitors for corrosion of 1018 carbon steel in nitric acid solution, *Corros. Sci.*, 48(2006), 1639-1654.

46. T. Salman, Q. Jawad, M. Hussain, A. Al-Amiery, L. Mohamed, A. Kadhum, M. Takriff, Novel ecofriendly corrosion inhibition of mild steel in strong acid environment: Adsorption studies and thermal effects, *Int. J. Corros. Scale Inhib.*, 8(2019), 1123-1137.

47. A. Alamiery, Effect of temperature on the corrosion inhibition of 4-ethyl-1-(4-oxo-4-phenylbutanoyl), *Lett. Appl. Nano. Bio. Sci.*, 11(2022), 3502-3508.

48. Alamiery, E. Mahmoudi, T. Allami, Corrosion inhibition of low-carbon steel in hydrochloric acid envi-ronment using a Schiff base derived from pyrrole: Gravimetric and computational studies, *Int. J. Corros. Scale Inhib.*, 10(2021), 749-765.

49. Alamiery, Corrosion inhibition effect of 2-N-phenylamino-5-(3-phenyl-3-oxo-1-propyl)-1, 3, 4-oxadiazole on mild steel in 1 M hydrochloric acid medium: Insight from gravimetric and DFT investigations, *Mater. Sci. Energy Technol.*, 4(2021), 398-406.

50. Alamiery, W. Wan Isahak, M. Takriff, M. S. Inhibition of mild steel corrosion by 4-benzyl-1-(4-oxo-4-phenylbutanoyl) thiosemicarbazide: gravimetrical, *Adsorp. Theoretical Stu. Lub.*, 9(2021), 93-104.

51. Jamil, A. Al-Okbi, M. Hanon, K. Rida, A. Alkaim, A. Al-Amiery, A. Kadhim, A. Kadhum, Carbethoxythiazole corrosion inhibitor: As an experimentally model and DFT theory, *J. Eng. Appl. Sci.*, 13(2018), 3952-3959.

52. S. Al-Baghdadi, T. Gaaz, A. Al-Adili, A. Al-Amiery, M. Takriff, Experimental studies on corrosion inhibition performance of acetylthiophene thiosemicarbazone for mild steel in HCl complemented with DFT investigation, *Int. J. Low-Carbon Technol.*, 16(2021), 181-188.

53. A. Al-Amiery, T. Salman, K. Alazawi, L. Shaker, A. Kadhum, M. Takriff, M.S. Quantum chemical elucidation on corrosion inhibition efficiency of Schiff base: DFT investigations supported by weight loss and SEM techniques, *Int. J. Low-Carbon Technol.*, 15(2020), 202-209.

54. T. Salman, K. Al-Azwi, I. Mohammed, S. Al-Baghdadi, A. Al-Amiery, T. Gaaz, A. Kadhum, Experimental studies on inhibition of mild steel corrosion by novel synthesized inhibitor complemented with quantum chemical calculations, Res. Phys., 10(2018), 291-296.

55. Zinad, Q. Jawad, M. Hussain, A. Mahal, L. Mohamed, A. Al-Amiery, Adsorption, temperature and corrosion inhibition studies of a coumarin derivatives corrosion inhibitor for mild steel in acidic medium: Gravimetric and theoretical investigations, *Int. J. Corros. Scale Inhib.*, 9(2020), 134-151.

56. Zinad, M. Hanoon, R. Salim, S. Ibrahim, A. Al-Amiery, M. Takriff, A. Kadhum, A.A. A new synthesized coumarin-derived Schiff base as a corrosion inhibitor of mild steel surface in HCl medium: Gravimetric and DFT studies, *Int. J. Corros. Scale Inhib.*, 9(2020), 228-243.

57. J.Yamin, E. Sheet, A. Al-Amiery, Statistical analysis and optimization of the corrosion inhibition efficiency of a locally made corrosion inhibitor under different operating variables using RSM, *Int. J. Corros. Scale Inhib.*, 9(2020), 502-518.

58. T. Salman, D. Zinad, S. Jaber, M. Al-Ghezi, A. Mahal, M. Takriff, A. Al-Amiery, Effect of 1,3,4-thiadiazole scaffold on the corrosion inhibition of mild steel in acidic medium: An experimental and computational study, *J. Bio-Tribo-Corros.*, 5(2019), 11-21.

59. M. Mohamed, A. Mahdy, R. Obaid, M. Hegazy, S. Kuo, K. Aly, Synthesis and characterization of polybenzoxazine/clay hybrid nanocomposites for UV light shielding and anti-corrosion coatings on mild steel, *J. Poly. Res.*, 28(2021), 1-15.

60. M. G. Mohamed, S. W. Kuo, A. Mahdy, I. M. Ghayd, K. I. Aly, Bisbenzylidene cyclopentanone and cyclohexanone-functionalized polybenzoxazine nanocomposites: Synthesis, characterization, and use for corrosion protection on mild steel, *Mater. Today Commun.*, 25(2020), 101418.

61. K. I. Aly, A. Mahdy, H. A. Hegazy, N.S. Al-Muaikel, S.W. Kuo, G. M. Mohamed, Corrosion resistance of mild steel coated with phthalimide-functionalized polybenzoxazines, *Coatings*, 10(2020), 1114.

62. K. I. Aly, M. Mohamed, O. Younis, M.H. Mahross, M. Abdel-Hakim, M. M. Sayed, Salicylaldehyde azine-functionalized polybenzoxazine: Synthesis, characterization, and its nanocomposites as coatings for inhibiting the mild steel corrosion, *Prog. Org. Coat.*, 138(2020), 105385.